

ELECTRON MOBILITY ON THE SURFACE OF LIQUID HELIUM: INFLUENCE OF SURFACE LEVEL ATOMS AND DEPOPULATION OF LOWEST SUBBANDS

*P. D. Grigoriev**, *A. M. Dyugaev*

*Landau Institute for Theoretical Physics
142432, Chernogolovka, Moscow Region, Russia*

*Max-Planck-Institut für Physik Komplexer Systeme
D-01187, Dresden, Germany*

E. V. Lebedeva

*Institute of Solid State Physics
142432, Chernogolovka, Moscow Region, Russia*

Received June 18, 2007

The temperature dependence of electron mobility is examined. We calculate the contribution to the electron scattering rate from the surface level atoms (SLA) proposed in [10]. This contribution is essential at low temperatures $T < 0.5$, when the He vapor concentration is exponentially small. We also study the effect of depopulation of the lowest-energy subband, which leads to an increase in the electron mobility at high temperature. The results obtained explain some long-standing discrepancies between the existing theory and experiment on electron mobility on the surface of liquid helium.

PACS: 73.20.-r, 68.03.-g, 73.40.-c, 67.90.+z, 68.03.Cd

1. INTRODUCTION

The two-dimensional electron gas on the surface of dielectric media is the subject of extensive research for several decades (see, e.g., [1–3] for reviews). The electrons are attracted to the interface by electric image forces and become localized in the direction perpendicular to the surface. The surface of liquid helium has no solid defects (impurities, dislocations, etc.) and gives a unique chance to create an extremely pure 2D electron gas. The electron mobility on the surface of liquid helium usually exceeds the electron mobility in 2D quantum wells in heterostructures by more than a thousand times. This system simulates the solid-state 2D quantum wells without disorder. Many fundamental properties of the 2D electron gas have been studied with the help of electrons on the surface of liquid helium. The many-body electron effects on the surface of liquid helium are determined by the interaction be-

tween electrons and surface waves (ripples) and by the Coulomb electron–electron (e – e) interaction screened by a substrate. The Wigner crystallization of the 2D electron gas, induced by the Coulomb e – e interaction, was first observed and extensively studied on the surface of liquid helium (see [1–3] for reviews). Various quantum electron objects (quantum dots [4], 1D electron wires [5], quantum rings [6], etc.) can be experimentally realized on the liquid helium surface. The electrons on the liquid helium surface may also serve for an experimental realization of a set of quantum bits with a very long decoherence time [7]. The electron properties in all these quantum systems depend in a crucial way on the structure and properties of the liquid helium surface itself.

The interface between liquid helium and the vacuum is usually supposed to be sharp: the number density of helium atoms decreases to zero over a distance of intermolecular spacing, which is much smaller than the size of the surface electron wave function. The electrons are clamped to the surface by the image force

*E-mail: grigoriev@itp.ac.ru

and by the external electric field. The electrons do not penetrate inside liquid helium because this penetration costs the energy $V_0 \approx 1$ eV. The total potential for the electrons on the surface of liquid helium can be written as [1–3]

$$V(z) = \begin{cases} -\Lambda/z + Fz, & z > 0, \\ V_0 \approx 1 \text{ eV}, & z < 0, \end{cases} \quad (1)$$

where $\Lambda \equiv e^2(\varepsilon - 1)/4(\varepsilon + 1)$, ε is the dielectric constant of helium, and $F = eE_\perp$ is the clamping electric field. Because the typical electron energy is of the order of temperature $T \ll V_0$, it is usually assumed that $V_0 = \infty$. The energy spectrum and the wave functions in potential (1) can be found only numerically. Without the external field ($F = 0$), the discrete energy levels and the electron wave functions are given by the same formula as in the hydrogen atom:

$$E_n = -\alpha/n^2, \quad n = 1, 2, \dots, \quad (2)$$

where $\alpha = m\Lambda^2/2\hbar^2$, and the electron wave function of the lowest-energy level in the z -direction is

$$\Psi_e(z) = 2\gamma^{3/2}z \exp(-\gamma z), \quad (3)$$

where $\gamma = m\Lambda/\hbar^2$. The dielectric constant of liquid helium is $\varepsilon_4 = 1.0572$, $\alpha_4 \approx 8$ K, and $\gamma = (76 \text{ \AA})^{-1}$ for ^4He and $\varepsilon_3 = 1.0428$, $\Lambda_3 = 1.205 \cdot 10^{-21}$ erg · cm, $\alpha_3 \approx 0.435$ K, and $\gamma = (101 \text{ \AA})^{-1}$ for ^3He . Hence, the electron wave function is rather extended in the z -direction, which reduces the influence of small surface ripples on the electron motion and makes the mobility of the 2D electrons gas on the helium surface rather high. At the low electron concentration $N_e \approx 10^7 \text{ cm}^{-2}$, the mobility of electrons on the liquid helium surface at $T = 0.1$ K reaches $10^4 \text{ m}^2/\text{V} \cdot \text{sec}$ [8], which is about 10^4 times greater than the highest electron mobility in heterostructures.

For several decades, the general opinion was that at sufficiently low temperatures, i.e., when the concentration of He vapor is exponentially small, the electrons on the surface of liquid helium interact with only one type of excitations, the quanta of surface waves, called ripplons. Therefore, the scattering on surface waves was believed to be the only mechanism determining the mobility, the cyclotron resonance linewidth, and other properties of surface electrons at temperature $T \lesssim 0.5$ K [1–3].

It has been known for 40 years that bound states of ^3He atoms may appear on the surface of liquid ^4He .

These surface bound states determine the value and the temperature dependence of the surface tension of a ^3He – ^4He mixture [9]. Recently, similar bound states were proposed [10] in the pure He isotopes and were called the surface level atoms (SLA). These SLA may be considered a new type of surface excitations of liquid He in addition to the ripplons. It is the SLA rather than ripplons that determine the temperature dependence of the surface tension of both liquid helium isotopes and provide an explanation to the long-standing puzzles [10, 11] in this temperature dependence [10]. In particular, the SLA explain the exponential temperature dependence of the surface tension of liquid ^3He at temperatures below 0.15 K. After taking SLA into account, a very good agreement (up to 0.1%) can be reached between theory and experiment on the temperature dependence of the He surface tension in a large temperature range [10].

An accurate microscopic description of this new type of excitations is a rather complicated many-particle problem. However, SLA can be considered phenomenologically, similarly to the quantum states of helium atoms localized above the liquid helium surface [10]. The SLA may also propagate in the surface plane and have the quadratic dispersion

$$\varepsilon(k) = E_{SLA} + k^2/2M^*,$$

where k is the 2D momentum of SLA along the surface. Both the SLA energy E_{SLA} and the effective mass M^* depend on the He isotope ^3He or ^4He . The SLA energies E_{SLA} are intermediate between the energy E_{vac} of a He atom in the vacuum and the chemical potential μ of this atom inside the liquid. If we take the energies of He atoms in the vacuum to be zero, $E_{vac}^{\text{He}} = 0$, the chemical potentials are $\mu^{4\text{He}} = -7.17$ K and $\mu^{3\text{He}} = -2.5$ K as $T \rightarrow 0$, while the energies of SLA, as suggested by the temperature dependence of the surface tension [10], are¹⁾

$$E_{SLA}^{4\text{He}} \approx -3.2 \text{ K} \text{ and } E_{SLA}^{3\text{He}} \approx -2.25 \text{ K}. \quad (4)$$

Therefore, at sufficiently low temperatures, the concentration of SLA becomes exponentially higher than the He vapor concentration, and the influence of the SLA

¹⁾ The value $E_{SLA}^{3\text{He}}$ is known quite accurately from the experiments on temperature dependence of surface tension $\sigma(T)$, since the latter is determined by SLA only [10]. For ^4He , there is a problem of separating the contributions from SLA and ripplons to $\sigma(T)$, and the value $E_{SLA}^{4\text{He}}$ can be determined with an accuracy about 1 K.

on the properties of surface electrons becomes more important than the influence of He vapor. Thus, the scattering on the surface level atoms affects the mobility, the quantum decoherence time, and other properties of surface electrons. This influence may give an additional experimental proof of the SLA existence and provide information on the SLA microscopic structure.

On the other hand, there is a long-standing discrepancy between the theory [12] of electron mobility on the liquid helium surface and the experimental data (see Fig. 2 in Ref. [8]). First, the measured electron mobility is usually lower than the theoretically predicted one. This deviation increases as the temperature decreases and suggests the existence of an additional scattering mechanism, which is important in the intermediate temperature range between the regions where the dominant scattering mechanisms are helium vapor atoms and ripples. Second, according to the existing theory [12], the ratio of electron mobilities on ^3He and ^4He surfaces at the same concentration of helium vapor must be equal to $\gamma^{4\text{He}}/\gamma^{3\text{He}} = 1.33$, where γ is determined by Eq. (3), but experiment shows that this ratio strongly depends on temperature even in the region where the scattering on helium vapor should be dominant [8]. The experimental lines (see Fig. 2 in Ref. [8]) even cross each other at the vapor density $N_v \approx 2 \cdot 10^{18} \text{ cm}^{-3}$. Other experiments with electrons on the helium surface also show a considerable inconsistency between theory and experiment. Thus, the theory in [13] predicts the shift of the cyclotron resonance frequency as a function of the clamping electric field 2–3 times less than the one experimentally measured in [14] (see [1, 2] for a review). The measured linewidth of the “vertical” (i.e., intersubband) electron transitions at low temperature is also considerably larger than the prediction of the theory.

In this paper, we only consider the electron mobility on the surface of liquid helium. We calculate the effect that the scattering on SLA has on the mobility of 2D surface electrons and analyze whether this influence can be experimentally separated from other contributions (such as the scattering on ripples and vapor atoms) and whether taking this influence into account helps to explain the existing discrepancy between theory and experiment. Similar surface states may also occur in other liquids and solids, such as solid hydrogen or neon, leading to similar questions. We also show that depopulation of the lowest-energy electron subband with an increase in temperature (quantum thermal evaporation) may explain the deviation of the measured electron mobility from the theory in [12] at high temperature.

2. ELECTRON SCATTERING ON HELIUM VAPOR AND ON SURFACE LEVEL ATOMS

Vapor atoms or SLA can be considered point-like impurities localized at points r_i . These impurities interact with electrons via a δ -function potential $V_i(r) = U\delta(r - r_i)$. Then there is no difference between the transport and the usual mean free time τ , which is given by

$$\frac{1}{\tau} = \frac{2\pi}{\hbar} \int dz N_{\text{He}}^{\text{tot}}(T, z) \times \int \frac{d^2\mathbf{p}'}{(2\pi\hbar)^2} |T_{\mathbf{p}\mathbf{p}'}(z)|^2 \delta(\epsilon_{\mathbf{p}} - \epsilon_{\mathbf{p}'}), \quad (5)$$

where $\epsilon(\mathbf{p}) = \mathbf{p}^2/2m^*$ is the electron dispersion relation, m^* is the effective electron mass, and $|v_{\mathbf{p}}| = p/m^*$ is the electron speed. The 2D matrix element of the electron scattering by helium atom is

$$T_{\mathbf{p}\mathbf{p}'}(z) = |\Psi_{\epsilon}(z)|^2 U.$$

The integration over \mathbf{p}' in (5) eliminates the delta-function, with the result

$$\frac{1}{\tau} = \int dz N_{\text{He}}^{\text{tot}}(T, z) \Psi_{\epsilon}^4(z) \frac{A\hbar\pi}{m}, \quad (6)$$

where $A = m^2 U^2 / \pi \hbar^4 = 4\pi f_0^2$ is the cross section of electron scattering on a He atom. The scattering amplitude f_0 of an electron by a helium atom is usually determined from the energy of the electron inside liquid helium, which is equal to $V_0 = 1 \text{ eV} = 2\pi\hbar^2 f_0^2 n_{\text{He}} / m_e$. At the He atom concentration $n_{\text{He}} = 2 \cdot 10^{22} \text{ cm}^{-3}$, this gives the scattering amplitude $f_0 = 0.62 \text{ \AA}$ and the cross section $A = 4.8 \text{ \AA}^2$ [1]. This value is in agreement with the direct measurements of the He atom cross sections [15].

The total density $N_{\text{He}}^{\text{tot}}(T, z)$ of helium atoms as a function of the distance to the surface is a sum of two parts:

$$N_{\text{He}}^{\text{tot}}(T, z) = N_v(T) + n_s(T, z). \quad (7)$$

The first part N_v is the density of helium vapor. It is roughly independent of z and is given by

$$N_v = \alpha \left(\frac{M k_B T}{2\pi\hbar^2} \right)^{3/2} \exp\left(\frac{\mu^{\text{He}} - E_{\text{vac}}^{\text{He}}}{k_B T} \right), \quad (8)$$

with the spin degeneracy $\alpha = 1$ for ^4He and $\alpha = 2$ for ^3He . The second part $n_s(z)$ is the density of SLA. It depends on the wave function $\Psi_s(z)$ of an atom on the surface level:

$$N_s(T, z) = n_s(T) \Psi_s^2(z). \quad (9)$$

The 2D SLA density $n_s(T)$ differs considerably for ^3He and ^4He [10]. For ^4He , it is given by the density of states of a 2D Bose gas:

$$n_{s4}(T) = \int \frac{d^2k}{(2\pi\hbar)^2} \frac{1}{\exp[(\varepsilon_4(k) - \mu^{4\text{He}})/T] - 1} = -\frac{M_4 T}{2\pi\hbar^2} \ln \left[1 - \exp\left(-\frac{\Delta_4}{T}\right) \right],$$

where $\Delta_4 = E_{SLA}^{4\text{He}} - \mu^{4\text{He}} \approx 4$ K is almost temperature independent and the SLA effective mass is $M_4 \approx 2.6 M_0^{4\text{He}}$. For ^3He , the SLA form a 2D Fermi gas with the density

$$n_{s3}(T) = 2 \int \frac{d^2k}{(2\pi\hbar)^2} \frac{1}{\exp[(\varepsilon_3(k) - \mu^{3\text{He}})/T] + 1} = \frac{M_3 T}{\pi\hbar^2} \ln \left[1 + \exp\left(-\frac{\Delta_3(T)}{T}\right) \right], \quad (10)$$

where $M_3 \approx 2.25 M_0^{3\text{He}}$ and

$$\Delta_3(T) = E_{SLA}^{3\text{He}}(T) - \mu^{3\text{He}}(T). \quad (11)$$

As $T \rightarrow 0$, $\Delta_3 = E_{SLA}^{3\text{He}} - \mu^{3\text{He}} \approx 0.25$ K [10]. The temperature dependence of the ^3He chemical potential $\mu^{3\text{He}}(T)$ is stronger than that for ^4He and may be essential even at low temperature [16, 17].

Assuming the electron scattering amplitude on vapor He atoms and on the SLA to be identical, we use (6) to calculate the electron mobility η_e as

$$\eta_e \approx \frac{\tau}{m} = \frac{1}{\pi\hbar A [N_v(T)I_v + n_s(T)I_s]}, \quad (12)$$

where we introduce the notation

$$I_s = \int \Psi_e^4(z) \Psi_s^2(z) dz \quad (13)$$

and

$$I_v = \int \Psi_e^4(z) dz. \quad (14)$$

In a weak clamping field $E_{\perp} \ll 200$ V/cm, we can take wave function (3) for the ground electron level, which gives

$$I_v \approx \int_0^{\infty} dz \left[2\gamma^{3/2} z \exp(-\gamma z) \right]^4 = 3\gamma/8. \quad (15)$$

In the absence of SLA, we then obtain [12]

$$\eta \approx \frac{8}{3\pi\hbar A \gamma N_v(T)}. \quad (16)$$

This estimate of the electron mobility is greater than the experimentally measured one by a constant factor about 2 [8], which stimulates the study of electron scattering by SLA.

To calculate the integral in (13), we must know the wave function $\Psi_s^2(z)$. An exact calculation of $\Psi_s(z)$ is a complicated many-particle problem. To estimate the contribution of scattering on surface atoms to the electron mobility, we can use an approximate wave function similar to the electron wave function in (4),

$$\Psi_s(z) = 2\gamma_s^{3/2} z \exp(-\gamma_s z) \quad (17)$$

(to be compared with (3)), with $\gamma_s = \sqrt{-2ME_{SLA}}/\hbar$, where E_{SLA} is the energy of the surface level and M is the free atom mass: $M^{4\text{He}} = 6.7 \cdot 10^{-24}$ g and $M^{3\text{He}} = 5.05 \cdot 10^{-24}$ g. This gives $\gamma_s^{4\text{He}} \approx (1.3 \text{ \AA})^{-1}$ and $\gamma_s^{3\text{He}} \approx (1.87 \text{ \AA})^{-1}$. Although the actual SLA wave function may differ from (17), as discussed below, trial function (17) follows the correct asymptotic behavior: it vanishes as $z \rightarrow 0$ and decreases exponentially as $z \rightarrow \infty$. With (17), we evaluate integral (13) as

$$I_s = \int 64\gamma_e^6 \gamma_s^3 z^6 \exp[-2(\gamma_s + 2\gamma_e)z] dz = \frac{360\gamma_s^3 \gamma_e^6}{(\gamma_s + 2\gamma_e)^7} \approx \gamma_e^2 \left[360 \left(\frac{\gamma_e}{\gamma_s} \right)^4 \right]. \quad (18)$$

The ratio

$$r \equiv \frac{n_s(T)I_s}{N_v(T)I_v} \approx \frac{n_s(T)}{N_v(T)} \frac{960\gamma_s^3 \gamma_e^5}{(\gamma_s + 2\gamma_e)^7} \quad (19)$$

may be less or greater than unity depending on the temperature and the clamping electric field. This ratio determines the role of SLA in the momentum relaxation of surface electrons. At low enough temperature, when the vapor atom density $N_v(T)$ is negligible compared with the SLA density because of the large negative exponent in (8), the ratio in (19) is much greater than 1. In the opposite limit of high temperature, when $\exp[(\mu^{\text{He}} - E_{vac}^{\text{He}})k_B T]$ in $N_v(T)$ is not negligibly small, the ratio is much less than 1 because of the second factor in the right hand side of Eq. (19), which contains the small factor $(\gamma_e/\gamma_s)^4 \sim 10^{-7}$.

This small factor $(\gamma_e/\gamma_s)^4$ in (18) indicates that the overlap of the electron and SLA wave functions $\Psi_e(z)$ and $\Psi_s(z)$ is small. The SLA wave function is located at a distance of the order of or less than 5 Å from the helium surface, while the electron wave function given by Eq. (3) vanishes at the surface. Therefore, integral (13) depends strongly on the behavior of the electron wave function near the helium surface. The surface electron

spectrum in (2) and the ground-state wave function (3) were calculated assuming that the potential barrier at the helium surface is infinite. As shown in [18], the electron spectrum could be changed distinctly if a finite value of the surface potential is taken into account. The finite height of this potential barrier shifts the electron wave function toward helium liquid $z < 0$, making its value at the surface considerably larger. On the other hand, due to the strong repulsion between two helium atoms at short distances, the actual SLA wave function is shifted outward from the surface by the distance $d \approx 1.5 \text{ \AA}$. It also depends on the density profile of liquid helium near its surface. We performed a numerical calculation of the electron wave function $\Psi_e(z)$ assuming a finite value of the potential $V(z)$ at the helium surface $z = 0$ and taking the clamping electric field into account. In calculating the SLA wave function $\Psi_s(z)$, we use the model potential

$$V_s(z) = \begin{cases} -\beta/z^3, & z > d, \\ +\infty, & z < d, \end{cases}$$

where β gives the correct asymptotic behavior at large distance, $\beta^{4\text{He}} = 117 \text{ K} \cdot \text{\AA}^3$ and $\beta^{3\text{He}} = 87.8 \text{ K} \cdot \text{\AA}^3$ ²⁾, and d is fitted to give the correct energy level value ($d^{3\text{He}} = 1.55 \text{ \AA}$ and $d^{4\text{He}} = 1.79 \text{ \AA}$). Then the integral in (13) becomes approximately 20 times larger than (18), being

$$I_{s3} \approx 4.3 \cdot 10^{-8} \text{ \AA}^{-2}, \quad I_{s4} \approx 1.3 \cdot 10^{-7} \text{ \AA}^{-2} \quad (20)$$

for ^3He and for ^4He correspondingly.

In a strong clamping electric field, the scattering rate of electrons increases due to an increase in the electron velocity in the z -direction: $v_{ze} \approx \hbar\gamma_e/m_e$ [2]. For the scattering on vapor atoms, this increase is slower than for the scattering on SLA and ripples. Because γ_e enters the ratio in (19) in the fifth power, the role of the scattering on SLA becomes more important in stronger clamping fields. It is impossible to analytically find the wave function of surface electrons in the presence of both the image potential and the clamping field. Approximate analytic estimates show that in a rather strong clamping field ($300 \text{ V/cm} < E_{\perp} < 10^5 \text{ V/cm}$), the scattering rate on vapor atoms increases as

$$I_v \propto \int \Psi^4(x) x \propto E_{\perp}^{1/3},$$

²⁾ These values of β correspond to the van der Waals attraction of an atom to the liquid helium distributed uniformly in the half-space: $\beta^{\text{He}} = (\pi/6) \alpha_6 n_{\text{He}}$, where $\alpha_6 \approx 1.02 \cdot 10^4 \text{ K} \cdot \text{\AA}^3$ is the coefficient in the Lennard-Jones potential [18] and the atom densities are $n^{3\text{He}} = 1.635 \cdot 10^{22} \text{ cm}^{-3}$ and $n^{4\text{He}} = 2.184 \cdot 10^{22} \text{ cm}^{-3}$.

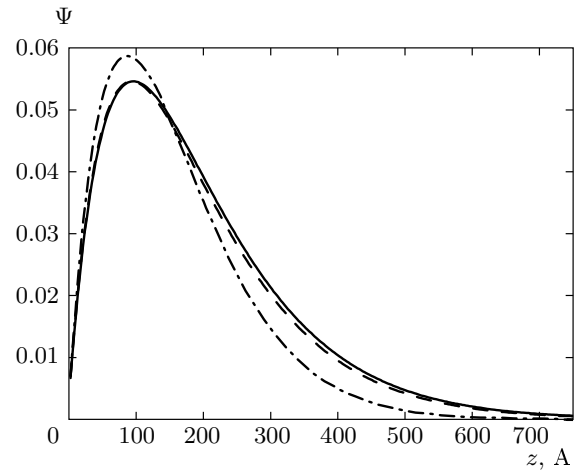


Fig. 1. The ground state electron wave function in the vicinity of the ^3He surface for three values of the clamping electric field: $E = 0$ (solid line), $E = 10 \text{ V/cm}$ (dashed line), and $E = 100 \text{ V/cm}$ (dashed-dotted line)

while the scattering on SLA increases stronger,

$$I_S \propto \Psi_e^4(1/\gamma_s) \propto E_{\perp}^{2/3}.$$

We note that the scattering rate on ripples in a strong field $E_{\perp} > 300 \text{ V/cm}$ is proportional to E_{\perp}^2 , i.e., the ripple contribution to the scattering rate in high field grows even stronger. The results of the numerical calculation for the electron wave function at different fields and for the integral $I_S(E_{\perp})$ with a finite value of the barrier V_0 in Eq. (1) are shown in Figs. 1 and 2.

In an approximate analysis, the variational method is traditionally used with the trial wave function (3), where

$$\gamma = \frac{\gamma_1}{3} \left[\frac{\gamma_0}{\gamma_1} + \left(1 + \sqrt{1 - \left(\frac{\gamma_0}{\gamma_1} \right)^6} \right)^{1/3} + \left(1 - \sqrt{1 - \left(\frac{\gamma_0}{\gamma_1} \right)^6} \right)^{1/3} \right] \quad (21)$$

is the variational parameter [1, 3] with $\gamma_1 = (\gamma_0^3 + 27\gamma_F^3/2)^{1/3}$, $\gamma_0 \equiv \gamma(E_{\perp} = 0)$, and $\gamma_F^3 = 3meE_{\perp}/2\hbar^2$. For the electron concentration $n_e = 1.21 \cdot 10^{27} \text{ cm}^{-3}$, as in the experiment on ^3He in Ref. [8], the minimum possible value of $eE_{\perp} = 2\pi e^2 n_e$ is approximately 10 V/cm . The actual clamping field for similar experiments was about 50 V/cm (see, e.g., [18]). The substitution of this value in (21) gives

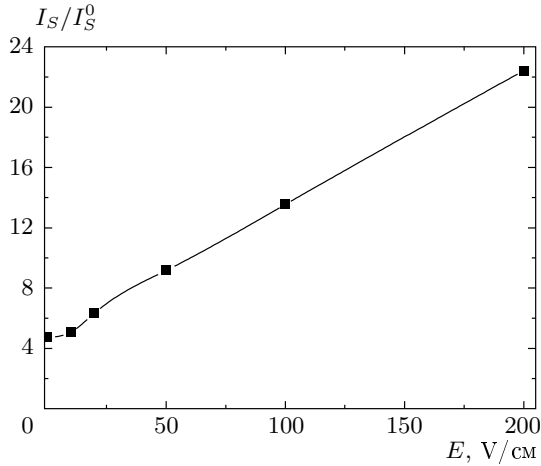


Fig. 2. Normalized scattering rate on SLA, which is proportional to integral (13), as a function of the clamping electric field. This figure shows that the scattering rate on SLA depends very strongly on the clamping field ($I_S = I_S(E)$ is calculated numerically taking the electron penetration under the barrier into account, and $I_S^0 = I_S(E = 0)$ is taken from Eq. (18))

$\gamma = \gamma_0$ with the accuracy of 6 decimal digits. But a numerical solution of the Schrödinger equation for the electron wave function under the conditions of this experiment shows that the electron wave function in the presence of an electric field differs perceptibly from the one in zero field. The results of the simulation for the electron above the ${}^3\text{He}$ surface is shown in Fig. 1. Because the electron wave function shrinks as the clamping field becomes stronger, the integral I_v in (14) increases and electron mobility (12) decreases. Our numerical results show that formula (21) is not valid for the intermediate clamping fields about 10–300 V/cm.

To compare the calculated mobility of electrons on the He surface with experiment, we have to take the electron scattering by ripples into account. The ripplon-limited mobility in a weak clamping field is given by the formula [1]

$$\eta_R = \frac{9\sigma\hbar^3}{m^2\Lambda^2\gamma^2T} \left[\frac{\text{cm}}{\text{dyn} \cdot \text{s}} \right], \quad (22)$$

and in a strong clamping field E_\perp it is

$$\eta_R = \frac{8\sigma\hbar}{m(eE_\perp)^2}. \quad (23)$$

The surface tension of ${}^4\text{He}$ is $\sigma_4 = 0.354$ dyn/cm, and

in the limit of weak clamping field, we obtain

$$\eta_R^{4\text{He}} \approx \frac{10^3}{k_B T} \left[\frac{\text{s}}{\text{g}} \right] = \frac{1.18 \cdot 10^7}{T [\text{K}]} \left[\frac{\text{cm}^2}{\text{V} \cdot \text{s}} \right]. \quad (24)$$

On the surface of liquid ${}^3\text{He}$, only short-wavelength ripples are suppressed by the high viscosity of the liquid (see Eqs. (26)–(29) in Ref. [10] for the criterion of damping of thermal ripples). But the leading contribution to electron scattering comes from long-wavelength ripples. Therefore, the ripplon contribution to the electron scattering on the surface of ${}^3\text{He}$ must be taken into account. The surface tension of ${}^3\text{He}$ is $\sigma_3 = 0.1557$ dyn/cm, and using Eq. (22) in the limit of weak clamping field, we obtain

$$\eta_R^{3\text{He}} \approx \frac{1390}{k_B T} \left[\frac{\text{s}}{\text{g}} \right] = \frac{1.6 \cdot 10^7}{T [\text{K}]} \left[\frac{\text{cm}^2}{\text{V} \cdot \text{s}} \right]. \quad (25)$$

The total electron mobility is

$$\eta_{tot}^{-1} = \eta_e^{-1} + \eta_R^{-1}, \quad (26)$$

where η_e^{-1} is given by Eq. (12). At sufficiently low temperatures, when the concentration of helium vapor is negligible and only scattering on ripples and SLA is important for ${}^4\text{He}$, Eqs. (12), (20), and (24) yield

$$\eta_{tot} = \frac{\eta_R}{1 + \eta_R/\eta_e} \approx \frac{\eta_R}{1 - \lambda_4 \ln[1 - \exp(-\Delta_4/T)]}, \quad (27)$$

where $\lambda_4 \approx 2$. For $T \ll \Delta_4$, this becomes

$$\eta_{tot} \approx \frac{\eta_R}{1 + \lambda_4 \exp(-\Delta_4/T)}.$$

Because $\Delta_4 \approx 4$ K, the contribution to electron scattering from the SLA on ${}^4\text{He}$ is negligible at all temperatures. It is much less than the contribution from vapor atoms for $T > 1$ K and much less than the contribution from ripples for $T < 1$ K.

The situation is different for ${}^3\text{He}$. Performing similar estimates, we then obtain

$$\eta_{tot} = \frac{\eta_R}{1 + \eta_R/\eta_e} \approx \frac{\eta_R}{1 + \lambda_3 \ln[1 + \exp(-\Delta_3/T)]}, \quad (28)$$

where $\lambda_3 \approx 1.4$. For $T \ll \Delta_3 \approx 0.25$ K, this becomes

$$\eta_{tot} \approx \frac{\eta_R}{1 + \lambda_3 \exp(-\Delta_3/T)},$$

while for $T \gg \Delta_3$, $\ln[1 + \exp(-\Delta_3/T)] \approx \ln 2$ and Eq. (28) becomes

$$\eta_{R+SLA} \approx \eta_R/2.$$

Therefore, the contribution of SLA to electron scattering on the ${}^3\text{He}$ surface can be detected from the temperature dependence of electron mobility in (28). The shift of the solid line with respect to the dashed line at low temperatures in Fig. 3 is due to the electron scattering by SLA.

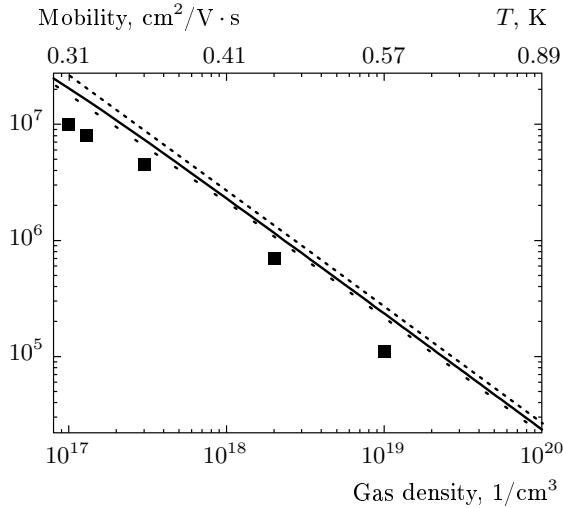


Fig. 3. The mobility of surface electrons as a function of the He vapor density for ^3He in a logarithmic scale. The dots are the experimental data in [8]. The dashed line is the theoretical prediction in [12]. The solid line is our modification of the results in [12] with the SLA contribution, the influence of the clamping electric fields $E = 50 \text{ V/cm}$ (solid line) and $E = 100 \text{ V/cm}$ (dotted line), and the penetration of the electron wave function under the finite potential barrier on the helium surface taken into account in calculating the electron scattering rate

3. DEPOPULATION OF THE LOWEST-ENERGY SUBBAND

As temperature increases, the occupation numbers of the higher-energy electron subbands also increase. The electron scattering rate on He atoms depends on the electron wave function $\Psi_e(z)$ and is the largest for the lowest subband (see Eqs. (14) and (13)). Therefore, the electron thermal evaporation from the lowest-energy subband increases the electron mobility. This effect can explain the deviation of experimental data at high temperature from Saitoh formula (16) (the upward curvature of the measured electron mobility at a high gas atom density in Fig. 2 in Ref. [8]).

At high temperature, the electrons scatter mainly on vapor atoms, and the total electron mobility is then calculated by the formula

$$\eta_e = \sum_{k=1}^{\infty} \frac{n_k}{\pi \hbar A N_v(T) I_k} \left(\sum_{k=1}^{\infty} n_k \right)^{-1}, \quad (29)$$

where $n_k = \exp(-E_k/T)$ are the occupation numbers of the ground-state and excited levels, $I_k \equiv \int \Psi_k^4(z) dz$, and $\Psi_k(z)$ is the eigenfunction of an electron on the

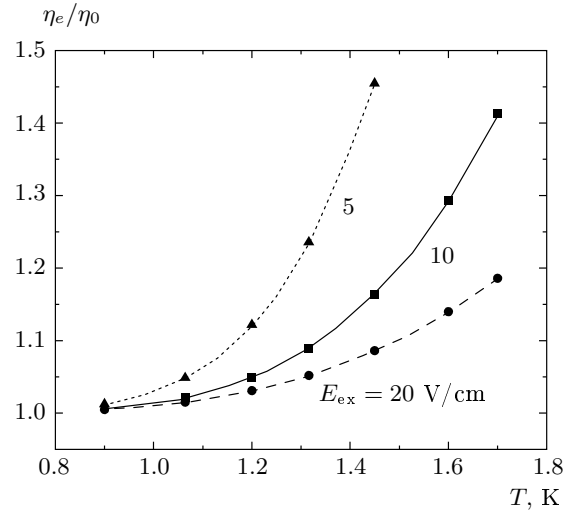


Fig. 4. The normalized sum $\eta_e/\eta_{e0} = \eta_e \pi \hbar A N_v(T) I_0 / n_0$ in (29) calculated for ^4He as a function of temperature at three different values of the external clamping field: $E_{ex} = 5, 10, 20 \text{ V/cm}$. This plot shows how great is the increase in the surface electron mobility due to the evaporation of electrons from the lowest subband

excited level. At high temperature, the total electron mobility (29) may differ considerably from the contribution $\eta_0 = [\pi \hbar A N_v(T) I_0]^{-1}$ of the ground level. We note that the sum in the numerator of Eq. (29) increases faster than the partition function in the denominator because of an extra factor $1/I_k$. For low electron levels, the external clamping field is a small correction to the image potential, and $1/I_k \sim k^2$ as in the hydrogen atom. For higher levels, the clamping field determines the electron wave function and $1/I_k \sim k^{2/3}$. Although the population of higher levels is not very large (about 0.01–0.05), the electrons on these levels contribute to the conductivity much more than the ground-level electrons. Evaluating sum (29) requires knowing the energy spectrum and the wave functions in potential (1). For an estimate of the sum in (29), we use the semiclassical approximation for all excited levels $k \geq 2$. For the ground energy level $k = 1$, a better accuracy is achieved using the exact solution of the Schrödinger equation in the absence of an external field, which gives $E_1 = -7.5 \text{ K}$. To check the results of the semiclassical calculation, we also calculated the sum in (29) using the numerical solution of the exact Schrödinger equation for the electron energy levels and the wave functions for the first three excited levels.

The result of the calculation of the sum in (29)

as a function of temperature is shown in Fig. 4 for three values of the clamping field: the field $E_{ex}^{sat} = 2\pi en_e = 10$ V/cm of saturation of the electron density in the experiment in Ref. [8], the field $E_{ex} = 20$ V/cm, and the field $E_{ex} = 5$ V/cm. The increase in the electron mobility on the helium surface $\Delta\eta_e$ depends strongly on temperature. At the clamping field $E_{ex}^{sat} = 10$ V/cm and the temperature $T = 1.3$ K, which corresponds to the ^4He vapor density $N_v = 10^{19}$ cm $^{-3}$, the calculated increase in the electron mobility due to evaporation from the lowest-energy level is $\Delta\eta_e \approx 10\%$ of the total mobility. This increase is not sufficiently large to agree quantitatively with the experimental data in Fig. 2 in Ref. [8]. In particular, the crossing of the calculated electron mobilities on ^3He and ^4He surfaces at $E_{ex} = 10$ V/cm occurs at the electron temperature $T_e \approx 1.6$ K, while in the experiment in Ref. [8], this crossing occurs at the vapor density $N_v \approx 2 \cdot 10^{18}$ corresponding to the temperature $T \approx 1.1$ K.

This discrepancy may occur for two reasons. First, the electron temperature T_e may differ from the helium temperature due to the heating of electrons by the electric field E_{\parallel} parallel to the surface, which is applied to study the electron mobility. The warm electrons leave the lowest-energy level and interact less with the helium vapor atoms and with ripplons. Hence, the energy relaxation of the warm electrons is not as fast as for the electrons on the lowest-energy subband. The problem of heating the electron system by the parallel electric field was considered in Refs. [19]. The electron temperature becomes considerably higher than the helium temperature at the field $E_{\parallel} \gtrsim 10^{-3}$ V/cm. The second reason could be the screening of the external electric field by other electrons. Assuming that the experiment in [8] was carried out in the saturation regime, i.e., with $E_{\perp} \approx 2\pi en_e$, the electric field well above the $2D$ layer of surface electrons is zero, because it is screened by the field $\Delta E_{\perp} = 2\pi en_e$ of the $2D$ layer of surface electrons. This screening is complete only for high electron levels with $\langle z \rangle_k \sim (n_e)^{-1/2}$ and $k \gtrsim 200$. However, even partial screening of the external electric field may drastically change the temperature dependence of the electron mobility (see the calculated electron mobility at $E_{ex} = 5$ V/cm plotted in Fig. 4). Because the partition function $\sum_k \exp(-E_k/T)$ diverges without an external field, the high levels may make an essential contribution to the electron mobility if the value of the clamping electric field corresponds to the saturation regime $E_{ex} = 2\pi en_e$. We see that the electron mobility on the helium surface at high temperature depends strongly on the applied electric field. Unfortu-

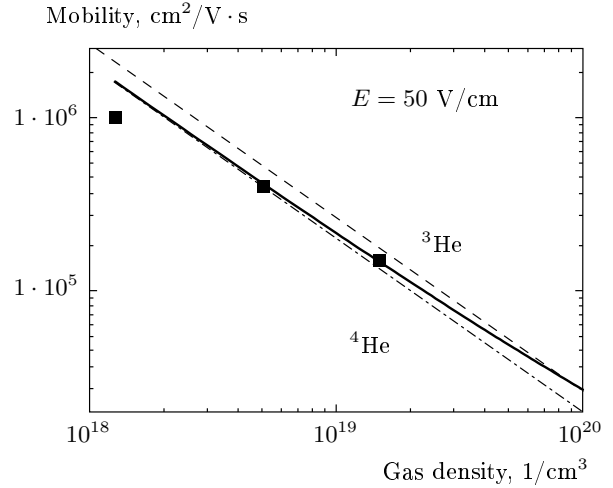


Fig. 5. The mobility of surface electrons as a function of the He vapor density in a logarithmic scale. The dots are the experimental data in [8]. The dashed lines are the theoretical prediction in [12] for ^4He and ^3He . The solid line represents the mobility of electrons above ^4He calculated with the population of three excited levels taken into account

nately, the clamping field is not specified in Ref. [8], and we cannot therefore make a quantitative comparison with the experimental data there. In Ref. [20], the electron mobility was measured in the saturation regime at the field $E_{\perp} = 30$ V/cm, and the deviation from the simple exponential temperature dependence in (16) was observed at $T > 0.85$ K, showing a substantial population of higher-energy levels at this temperature. In the experiment in Ref. [21], performed at $E_{\perp} = 200\text{--}400$ V/cm, no considerable deviation from the exponential temperature dependence of the electron mobility was observed up to $T \approx 2$ K. We note that the electron mobility measured in Ref. [21] is also less than the prediction following from Eq. (16) by a constant factor about 4 in the entire temperature range.

In Fig. 5, we show the results of calculation of the electron mobility above ^4He at the clamping field $E_{\perp} = 50$ V/cm considerably stronger than the saturation field $E_{sat} = 10$ V/cm in experiment [8]. The figure demonstrates an increase in the mobility with respect to the Saitoh results and a better agreement with experiment in this temperature range. This evaluation underestimates the effect of the electron evaporation from the lowest-energy subband because it does not take the screening of the clamping electric field by surface electrons into account. The accurate calculation of the screening effect may substantially improve the agreement with experiment.

4. CONCLUSION

To summarize, we investigated the two effects that influence the mobility of electrons on the surface of liquid helium.

First, we studied the electron scattering by the new type of excitations, recently proposed in Ref. [10] and called surface level atoms (SLA). The electron scattering by SLA is reduced by the small overlap between the wave functions of electrons and SLA. It turns out to be negligible for electrons on the surface of liquid ^4He . Electron scattering on SLA is only essential on the ^3He surface at temperatures below 0.4 K, when the concentration of helium vapor is exponentially small. The electron scattering rate on SLA increases with an increase in the clamping electric field. The temperature and clamping field dependence of the SLA contribution to the electron scattering differs considerably from that of ripplon scattering (see Eq. (28)). Therefore, the electron scattering by SLA can be separated from the experimental data on electron mobility above ^3He , which can provide an additional proof of the existence of SLA (currently, the only experimental substantiation of the SLA existence comes from the temperature dependence of the surface tension of liquid He [10]). The contribution from the SLA improves the agreement between theory and experiment as regards the surface electron mobility (see Fig. 3). But this contribution alone is not sufficient to explain all puzzles in the temperature dependence of the surface electron mobility. For example, it does not explain the electron mobility two times smaller than predicted in the paper [12] at a temperature about (0.5–1) K when only the scattering by vapor atoms should be essential. A quantitative estimate of the contribution of SLA to the surface electron scattering rate requires a more profound study of the microscopic structure of SLA. We leave this study for future publications, showing only that the SLA may considerably change the surface electron mobility in a certain temperature range. The SLA may also affect other properties of the surface electrons, such as the cyclotron resonance line width and the quantum decoherence time of surface electrons in various configurations. In particular, the SLA may considerably influence the properties of quantum electron states on the helium surface in the confining in-plane potential. Since the ripplon-limited width of the electron transitions between localized states in quantum dots on the surface of liquid helium is much smaller than the level width of delocalized electrons [22–24], the contribution to the level broadening and to the quantum decoherence time from the SLA could be dominant.

At high temperatures, $T > 1$ K for ^4He and $T > 0.7$ K for ^3He , the evaporation of electrons from the lowest energy subband may become essential. This evaporation leads to a considerable increase in the electron mobility, which depends strongly on the temperature and on the external clamping field (see Fig. 4). This evaporation explains the increase in the measured electron mobility [8] at high temperature compared to Saitoh formula (16). This evaporation also explains the crossing of the mobility graphs of ^3He and ^4He as functions of the He vapor concentration, which in the experiment in [8] occurs at $N_v \approx 2 \cdot 10^{18}$. Quantitative results of the temperature dependence of the electron mobility depend very strongly on the value of the clamping electric field, which is not given in Ref. [8]. Therefore, we perform only a qualitative comparison with the experimental data on the temperature dependence of electron mobility.

The work was supported by the RFBR (grants №№ 06-02-16551, 06-02-16223).

APPENDIX

Semiclassical calculation of energy levels and electron wave functions

The Bohr–Zommerfeld quantization rule with potential (1) can be written as

$$\int_0^{\tilde{z}} dx \sqrt{2m \left(E_n - Fx + \frac{\Lambda}{x} \right)} = \pi \hbar \left(n - \frac{1}{4} \right), \quad (\text{A.1})$$

where the turning point is determined by

$$\tilde{z} = \frac{E_n}{2F} + \sqrt{\left(\frac{E_n}{2F} \right)^2 + \frac{\Lambda}{F}}.$$

The semiclassical wave functions are

$$\Psi(z) = \frac{C}{\sqrt{p}} \begin{cases} \cos \left\{ \frac{1}{\hbar} \left| \int_{\tilde{z}}^z p dz \right| - \frac{\pi}{4} \right\}, & z < \tilde{z}, \\ \frac{1}{2} \exp \left\{ \frac{-1}{\hbar} \left| \int_{\tilde{z}}^z p dz \right| \right\}, & z > \tilde{z}. \end{cases} \quad (\text{A.2})$$

The electron momentum is given by

$$p(z) \equiv \sqrt{2m |E - V(z)|},$$

where the potential $V(z)$ is given by Eq. (1).

Introducing the normalized coordinate and energy

$$x_1 = x\sqrt{F/\Lambda}, \quad E^* \equiv E/\sqrt{F\Lambda},$$

we rewrite Eq. (A.1) as

$$a_1 \int_0^{\tilde{z}_1} dx_1 \sqrt{E_n^* - x_1 + 1/x_1} = \left(n - \frac{1}{4}\right), \quad (\text{A.3})$$

$$\tilde{z}_1 = \frac{E_n^*}{2} + \sqrt{\left(\frac{E_n^*}{2}\right)^2 + 1},$$

where for the external field corresponding to the saturation of the electron density $E_{ex} = 2\pi en_e = 10$ V/cm,

$$a_1 \equiv \frac{\sqrt{2m}}{\pi\hbar} \frac{(\Lambda)^{3/4}}{F^{1/4}} \approx 1.54.$$

The integral in (A.3) can be expressed in terms of elliptic integrals, and Eq. (A.3) can easily be solved numerically. The solution of this equation fits the dependence $E_k = C_1(k - C_2)^{2/3}$ with high accuracy starting from $k = 4$ for the field $E_{ex} > 5$ V/cm. The constant $C_1 \sim (E_{ex})^{2/3}$ in the absence of the image potential. The accuracy of the semiclassical approximation increases with the level number and is about 5% for the second energy level. The calculation of $I_k \equiv \int \Psi_k^4(z) dz$ was performed using wave functions (A.2). For the lowest three levels, the dependence $I_k \approx I_1/k^2$ corresponding to the absence of the external field is satisfied only very roughly. For higher levels ($k \geq 4$), the dependence $I_k \sim k^{-2/3}$ is satisfied with high accuracy, which corresponds to the absence of the image potential. The semiclassical approximation allows an easy numerical calculation of the sum in (29) with a very large number of energy levels.

REFERENCES

1. V. B. Shikin and Yu. P. Monarkha, *Two-Dimensional Charged Systems in Helium* (in Russian), Nauka, Moscow (1989).
2. V. S. Edel'man, *Sov. Phys. — Uspekhi* **130**, 676 (1980).
3. Y. Monarkha and K. Kono, *Two-Dimensional Coulomb Liquids and Solids*, Springer-Verlag (2004).
4. G. Papageorgiou, P. Glasson, K. Harrabi et al., *Appl. Phys. Lett.* **86**, 153106 (2005).
5. B. A. Nikolaenko, Yu. Z. Kovdrya, and S. P. Gladchenko, *J. Low Temp. Phys.* **28**, 859 (2002).
6. A. M. Dyugaev, A. S. Rozhavskii, I. D. Vagner, and P. Wyder, *JETP Lett.* **67**, 434 (1998).
7. P. M. Platzman and M. I. Dykman, *Science* **284**, 1967 (1999); M. I. Dykman, P. M. Platzman, and P. Seddighrad, *Phys. Rev. B* **67**, 155402 (2003).
8. K. Shirahama, S. Ito, H. Suto, and K. Kono, *J. Low Temp. Phys.* **101**, 439 (1995).
9. A. F. Andreev, *Zh. Eksp. Teor. Fiz.* **50**, 1415 (1966) [*Sov. Phys. JETP* **23**, 939 (1966)].
10. A. M. Dyugaev and P. D. Grigoriev, *JETP Lett.* **78**, 466 (2003).
11. M. Iino, M. Suzuki, A. J. Ikushima, and Y. Okuda, *J. Low Temp. Phys.* **59**, 291 (1985); M. Suzuki, Y. Okuda, A. J. Ikushima, and M. Iino, *Europhys. Lett.* **5**, 333 (1988); K. Matsumoto, Y. Okuda, M. Suzuki, and S. Misawa, *J. Low Temp. Phys.* **125**, 59 (2001).
12. M. Saitoh, *J. Phys. Soc. Jpn.* **42**, 201 (1977).
13. A. Cheng and P. M. Platzman, *Sol. State Comm.* **25**, 813 (1978); V. B. Shikin, *Zh. Eksp. Teor. Fiz.* **77**, 717 (1979) [*Sov. Phys. JETP* **50**, 360 (1979)]; M. I. Dykman and L. S. Khazan, *Zh. Eksp. Teor. Fiz.* **77**, 1488 (1979) [*Sov. Phys. JETP* **50**, 747 (1979)].
14. V. S. Edel'man, *Zh. Eksp. Teor. Fiz.* **77**, 673 (1979) [*Sov. Phys. JETP* **50**, 338 (1979)].
15. D. E. Golden and H. W. Bandel, *Phys. Rev.* **138**, A14 (1965); L. S. Frost and A. V. Phelps, *Phys. Rev.* **136**, A1538 (1964).
16. A. M. Dyugaev, *J. Low Temp. Phys.* **78**, 79 (1990).
17. A. M. Dyugaev, *Sov. Sci. Rev. A. Phys.* **14**, 1 (1990).
18. C. C. Grimes, T. R. Brown, Michael L. Burns, and C. L. Zipfel, *Phys. Rev. B* **27**, 140 (1976).
19. R. S. Crandall, *Phys. Rev. B* **12**, 119 (1975); V. B. Shikin and Yu. P. Monarkha, *J. Low Temp. Phys.* **16**, 193 (1974); M. Saitoh, *J. Phys. Soc. Jpn.* **42**, 201 (1977); M. Saitoh and T. Aoki, *J. Phys. Soc. Jpn.* **44**, 71 (1978); T. Aoki and M. Saitoh, *J. Phys. Soc. Jpn.* **46**, 423 (1979); Yu. P. Monarkha, *Fiz. Nizkikh Temp.* **5**, 994 (1979); M. Saitoh, T. Aoki, *Surf. Sci.* **98**, 61 (1980).
20. C. C. Grimes and G. Adams, *Phys. Rev. Lett.* **36**, 145 (1976).
21. W. T. Sommer and D. J. Tanner, *Phys. Rev. Lett.* **27**, 1345 (1971).
22. P. D. Grigor'ev, *Pis'ma Zh. Eksp. Teor. Fiz.* **66**, 599 (1997) [*JETP Lett.* **66**, 630 (1997)].
23. P. D. Grigoriev and A. M. Dyugaev, *JETP* **93**, 103 (2001).
24. M. I. Dykman, P. M. Platzman, and P. Seddighrad, *Phys. Rev. B* **67**, 155402 (2003).